

CHALLENGES OF NUCLEAR STRUCTURE

Proceedings of the 7th International Spring Seminar on Nuclear Physics

Maiori, Italy

27-31 May 2001

edited by

Aldo Covello

*Dipartimento di Scienze Fisiche
Università di Napoli Federico II*

 **World Scientific**
Singapore • New Jersey • London • Hong Kong

References

1. N. V. Giai, Ch. Stoyanov, V. V. Voronov, *Phys. Rev. C*, *Phys. Rev. C* **57**, 1204 (1998).
2. V. O. Nesterenko, J. Kvasil, P.-G. Reinhard, W. Kleinig, these proceedings.
3. D. Vautherin, *Phys. Rev. C* **7**, 296 (1973).
4. G. F. Bertsch, S. F. Tsai, *Phys. Rep.*, *Phys. Lett.* **18C** (1975) 126.
5. N. V. Giai, H. Sagawa, *Phys. Lett. B* **106**, 379 (1981).

QUADRUPOLE DEFORMATIONS OF DRIP-LINE NUCLEI .

M.V. STOITSOV,¹ J. DOBACZEWSKI,² W. NAZAREWICZ,^{2,3} AND S. PITTEL⁴

Institute of Nuclear Research and Nuclear Energy, Bulgarian Academy of Sciences, Sofia-1 784, Bulgaria

²*Institute of Theoretical Physics, Warsaw University, Hoza 69, PL-00-681 Warsaw, Poland*

³*Department of Physics and Astronomy, University of Tennessee, Knoxville, Tennessee 37996*

Physics Division, Oak Ridge National Laboratory, Oak Ridge, Tennessee 37831

⁴*Bartol Research Institute, University of Delaware, Newark, Delaware 19716*

The Hartree Fock Bogolyubov method in a Transformed Harmonic Oscillator basis (HFB+THO) is presented as a practical tool for axially deformed configuration-space calculations. It is shown that the HFB+THO results almost exactly reproduce those of coordinate-space HFB calculations for spherical and axially deformed nuclei. The HFB+THO procedure, as currently formulated, is fully automated, thereby facilitating the systematic investigation of large sets of nuclei.

1 Introduction

Recent advances in radioactive ion beam technology have opened up the possibility of exploring very weakly-bound nuclei in the neighborhood of the particle drip lines¹. A framework for a reliable theoretical description of such exotic nuclei is provided by coordinate-space Hartree-Fock-Bogoliubov (HFB) theory². Serious difficulties arise, however, when this methodology is applied to deformed nuclei³.

In the absence of reliable coordinate-space solutions to the deformed HFB equations, it is useful to consider instead the configuration-space approach, whereby the HFB solution is expanded in a complete single-particle basis. This method, with an expansion in a harmonic oscillator basis (HFB+HO), has been applied extensively in nuclear physics using Skyrme forces, the Gogny effective interaction, or in calculations based on a relativistic Lagrangian. For nuclei at the drip lines, however, the HFB+HO expansion converges much too slowly², producing wave functions that decrease too steeply at large distances.

An alternative approach has recently been proposed whereby the quasi-particle HFB wave functions are expanded in a complete set of Transformed Harmonic Oscillator (THO) wave functions⁴ obtained by applying a local-scaling coordinate transformation 'LST' to the standard HO basis. The THO basis preserves many useful properties of the HO wave functions, but in addition gives us access to the precise form dictated by the desired asymptotic behavior of the densities.

Applications of this new HFB+THO methodology have been reported both in the non-relativistic and relativistic domains⁴. In all of these calculations, specific global parametrizations were employed for the scalar LST function that defines the THO basis. Several points in such an approach require special attention: (i) Any global parameterization of the LST function modifies properties throughout the entire nuclear volume in order to improve the asymptotic density at large distances. This is not necessary, however, since the HFB+HO results are usually reliable in the nuclear interior; even for weakly-bound systems. (ii) Because of the matching conditions between the interior and exterior regions, the global LST function has a complicated behavior, especially around the classical turning point, and therefore it cannot be easily parameterized with a simple expression. (iii) The minimization procedure applied to optimize the basis parameters becomes very time consuming, especially when a large number of shells are included. Also, in some cases, the minimization algorithm is ill-behaved and thus does not bring any substantial improvement in precision.

In the present work, we study how to better define the THO basis for a practical and reliable HFB+THO theory of weakly-bound nuclei far from closed shells. We first examine carefully the differences between the results that emerge from coordinate-space HFB and configuration-space HFB+HO calculations for spherical nuclei. We will see that it is possible to precisely define the region where HFB+HO starts to deviate from the coordinate-space HFB solution. Based on this observation, one can propose a prescription for a correct continuation of the HFB+HO density by introducing the LST function. The resulting THO basis leads to HFB+THO results which almost exactly reproduce the coordinate HFB results for spherical nuclei² and the axially deformed nuclei⁶. The new method is naturally suited for systematic investigations of nuclear properties of weakly bound systems.

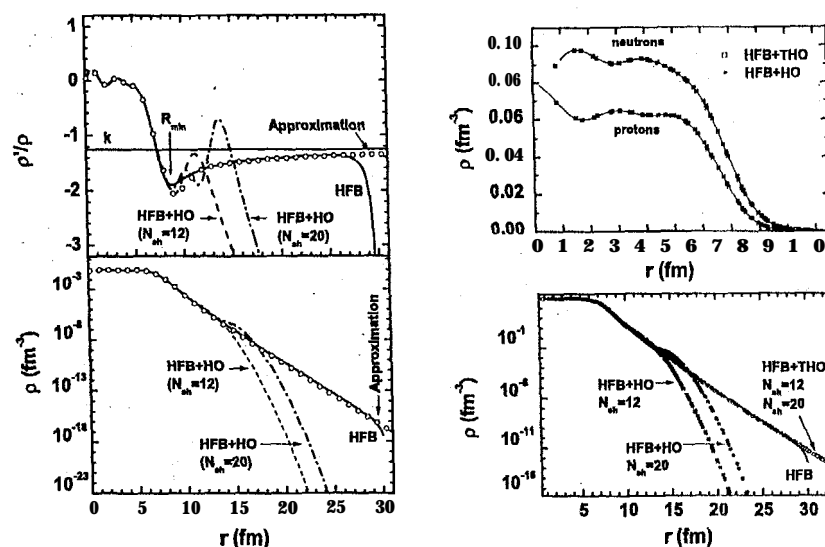


Figure 1. Left: logarithmic derivative of the density (upper panel), and the density in the logarithmic scale (lower panel), as functions of the radial distance. The coordinate-space HFB results (solid line) are compared with those for the HFB+HO method with $N_{sh}=12$ and 20 HO shells, as well with the approximation given by Eq. (6) (small circles). Right: comparison of the HFB+HO (closed symbols) and HFB+THO (open symbols) densities in the linear (upper panel) and logarithmic (lower panel) scales. Though the calculations were carried out for a specific nucleus and Skyrme interaction, the features exhibited are generic.

2 New representation of the LST function

2.1 Coordinate versus configurational HFB calculations

The main differences between coordinate HFB and configurational HFB+HO results can be seen clearly in plots of the associated local density distributions. A typical example is shown in the left part of Fig. 1 where the densities and their logarithmic derivatives from coordinate-space HFB calculations are compared with those from the configurational HFB+HO method.

Invariably the logarithmic derivative ρ'/ρ associated with the coordinate-space HFB solution shows a well-defined minimum around some point R_{min} in the asymptotic region, after which it smoothly approaches the constant value

$k=2\kappa$, where

$$\kappa = \sqrt{2m(E_{\min} - \lambda)/\hbar^2}, \quad (1)$$

is associated with the HFB asymptotic behaviour for the lowest quasiparticle state that has the corresponding quasiparticle energy E_{\min} (see Ref.²). This property is clearly seen in the upper left panel of Fig. 1. One can also see that the HFB+HO densities and logarithmic derivatives are in almost perfect agreement with the coordinate-space results up to (or around) the distance R_{\min} . Consequently, we conclude that the HFB+HO densities are numerically reliable up to that point.

Moreover, the HFB value of the density decay constant k , when calculated from Eq. (1), is also correctly reproduced by the HFB+HO results. It is not possible to distinguish between the values of k that emerge from the coordinate-space and harmonic-oscillator HFB calculations, both values being shown by the same line in the upper left panel of Fig. 1.

Soon beyond the point R_{\min} , the HFB+HO density begins to deviate dramatically from the coordinate-space results. When the number of harmonic oscillator shells N_{sh} is increased, the logarithmic derivative of the HFB+HO density develops oscillations around the exact solution. As a result, the logarithmic derivative of the HFB+HO density is very close to the coordinate-space result around the mid point $R_m = (R_{\max} - R_{\min})/2$, where R_{\max} is the position of the first maximum of the logarithmic derivative after R_{\min} .

In summary, the following HFB+HO quantities agree with the coordinate-space HFB results: (i) the value of the density decay constant k ; (ii) the local density up to the point R_{\min} where the logarithmic derivative ρ'/ρ shows a clearly-defined minimum; (iii) the actual value of this point R_{\min} ; (iv) the value of the logarithmic derivative of the density at the point R_m defined above. In fact, the last of the above is not established nearly as firmly as the first three; nevertheless, we shall make use of it in developing the new formulation of the HFB+THO method.

Beyond the point R_m , the HFB+HO solution fails to capture the physics of the coordinate-space results, especially in the far asymptotic region. It is this incorrect large- r behavior that we will now try to cure by introducing the THO basis.

2.2 Approximation to HFB local densities

Our goal is to try to find an approximation to the *exact* (coordinate-space) HFB density that is based only on information contained in the HFB+HO results. For this purpose, one can use the WKB asymptotic solution of the

single-particle Schrödinger equation for a given potential $V(r)$, under the assumption that beyond the classical turning point only the state with lowest decay constant κ contributes to the local density. Under this assumption, the logarithmic derivative of the density can be written as

$$\left. \frac{\rho'(r)}{\rho(r)} \right|_{r \rightarrow \infty} = -\frac{2}{r} - \sqrt{k^2 + 4V} - \frac{2V'}{k^2 + 4V}, \quad (2)$$

where the first term comes from the three-dimensional volume element, while the next two terms correspond to the first and the second order WKB solutions. The reduced potential \mathcal{V} ,

$$\mathcal{V}(r) = \frac{2m}{\hbar^2} V(r) = \mathcal{V}_N + \frac{\ell(\ell+1)}{r^2} + \frac{2mZe^2}{\hbar^2 r}, \quad (3)$$

is the sum of the nuclear, centrifugal, and Coulomb (for protons) contributions, where ℓ is the multipolarity of the particular state. In practical applications it turns out that near R_m the next-to-lowest quasiparticle states do still contribute to the local density ρ , and this effect is much more important than the second-order WKB term shown in Eq. (2). Therefore, we use the asymptotic approximation that has the form

$$\left. \frac{\rho'(r)}{\rho(r)} \right|_{r \rightarrow \infty} = -\frac{2}{r} - \sqrt{k^2 + 4V + C/r^2}. \quad (4)$$

Since the decay constant k is known from the HFB+HO calculation, and assuming that the nuclear part \mathcal{V}_N is small, we are left with only one redefined phenomenological parameter C in the logarithmic derivative. One can fix the actual value of C from the condition that the logarithmic derivative (4) coincides with the HFB+HO result at the mid point R_m . Then, in order to make a smooth transition from the HFB+HO density $\bar{\rho}(r)$ in the inner region to the approximate asymptotic expression (4) in the outer region, we introduce the following representation for the logarithmic density derivative:

$$\frac{\bar{\rho}'(r)}{\bar{\rho}(r)} = \begin{cases} \frac{\rho'(r)}{\rho(r)} & \text{for } r \leq R_{\min} \\ -a + b(R_{\min} - r)^2/r^m & \text{for } R_{\min} \leq r \leq R_{\max} \\ -\frac{2}{r} - \sqrt{k^2 + 4V + C/r^2} & \text{for } r \geq R_{\max} \end{cases} \quad (5)$$

The constants a , b and m are determined from the condition that the logarithmic derivative of the density (5) and its first derivative be smooth functions at R_{\min} and R_{\max} . Notice that the first derivative of (5) at R_{\min} is automatically zero so that there is no need to introduce a fourth parameter to satisfy this condition.

Having determined a smooth expression for $\tilde{\rho}'(r)/\tilde{\rho}(r)$ and its first derivative, we can derive a corresponding approximate expression for the local density distribution $\tilde{\rho}(r)$ by simply integrating Eq. (5). The result is

$$\tilde{\rho}(r) = \begin{cases} \tilde{\rho}(r) & \text{for } r \leq R_{\min} \\ Ae^{-\alpha r} \exp \left[\frac{b}{r^{1-m}} \left(\frac{br^2}{3-m} - \frac{2rR_{\min}}{2-m} + \frac{R_{\min}^2}{1-m} \right) \right] & \text{for } R_{\min} \leq r \leq R_{\max} \\ Br^{-2} \exp \left(-\int_r^{\infty} \sqrt{k^2 + 4V(x)} dx \right) & \text{for } r \geq R_{\max} \end{cases} \quad (6)$$

where the integration constants A and B are determined from a matching condition for the density at the points R_{\min} and R_{\max} , respectively. Finally, $\tilde{\rho}(r)$ should be normalized to the appropriate particle number.

The approximation $\tilde{\rho}(r)$ works fairly well for all nuclei that we have considered. As seen in Fig. 1, the density that emerges from prescription (6) is in perfect agreement with the coordinate-space HFB results.

2.3 LST function for HFB+THO calculations

The starting point of our new and improved HFB+THO procedure is thus to carry out a standard HFB+HO calculation for the nucleus of interest, thereby generating its local density, and then to use the method outlined in the previous section to correct that density in the large- r regime [see Eq. (6)]. The HFB+HO density can be expressed as an expansion in the HO basis according to

$$\tilde{\rho}(\mathbf{r}) = \sum_{\alpha\beta} \tilde{\rho}_{\alpha\beta} \varphi_{\alpha}^*(\mathbf{r}) \varphi_{\beta}(\mathbf{r}). \quad (7)$$

The next step is to define the LST⁴ so that it transforms the HFB+HO density (7) into the corrected density of Eq. (6). This requirement leads to the following first-order differential equation,

$$\tilde{\rho}(\mathbf{r}) \frac{f^2(\mathcal{R})}{\mathcal{R}^{2n}} \frac{\partial f(\mathcal{R})}{\partial \mathcal{R}^2} \left(\frac{\mathbf{r}}{\mathcal{R}} f(\mathcal{R}) \right), \quad (8)$$

which for spherical densities and the initial condition $f(0) = 0$ can always be solved for $f(\mathcal{R})$. In the case of axially-deformed nuclei, we instead carry out a Legendre expansion of the deformed HFB+HO local density in terms of the spherically symmetric components $\tilde{\rho}_l(r)$. Only the scalar component, $\tilde{\rho}_{l=0}(r)$, has the normalization of the total density distribution. Therefore, in the case of deformed nuclei, we use $\tilde{\rho}_{l=0}(r)$ in Eq. (8) to define the LST function $f(\mathcal{R})$.

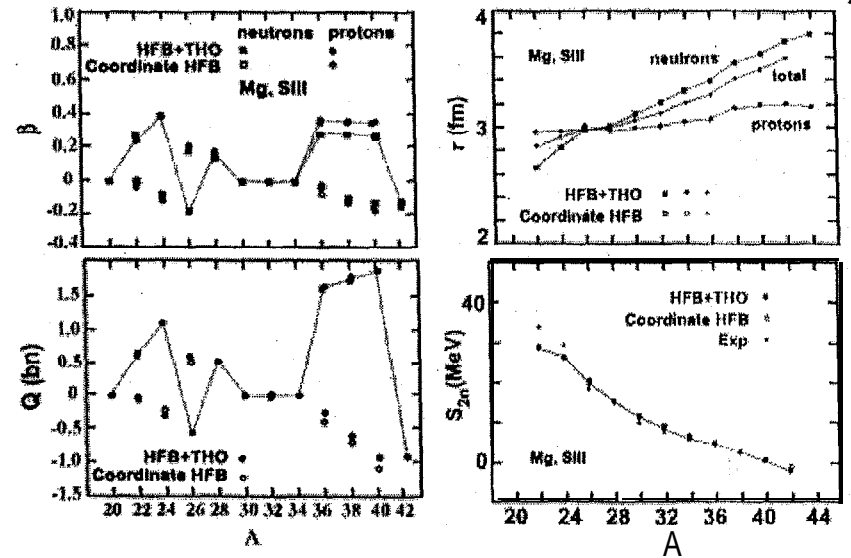


Figure 2. Comparison of HFB+THO results (black symbols) with the results of Terasaki et al. (open symbols) for the quadrupole deformations (upper left panel), quadrupole moments (lower left panel), rms radii (upper right panel) and S_{2n} values (lower right panel) within the Mg chain.

In this way, the solution $f(\mathcal{R})$ of Eq. (8) generates a THO basis that when applied to the HFB+HO density $\tilde{\rho}_{\alpha\beta}$ leads to the corrected density $\tilde{\rho}(r)$ which has proper asymptotic behavior. Most importantly, no information is required to build the THO basis beyond the results of a standard HFB+HO calculation. Since no further parameters enter, there is no need to minimize the HFB+THO total energy. As a consequence, with this new methodology we are able to systematically treat large sets of nuclei within a single calculation.

3 Comparison with available coordinate-space HFB results

3.1 Comparison for spherical nuclei

We have performed configurational HFB+THO calculations for a number of spherical nuclei. Sample results are compared with those from coordinate-

space HPB calculations? in the right panels of Fig. 1. As expected, the HFB+THO results are in excellent agreement with the exact HFB results. This and other comparisons we have carried out suggest the usefulness of the THO basis in configuration-space HFB calculations of weakly-bound systems.

3.2 Comparison for axially deformed nuclei

Coordinate-space discretization algorithms become technically very complicated when applied to deformed nuclei. It is therefore very difficult to carry out comparisons of the HFB+THO formalism with exact coordinate-space results in such nuclei. So far, there has only been one chain of nuclei – the even Mg isotopes – that has been systematically investigated in the coordinate-space framework, by combining the imaginary-time evaluation method with a diagonalization of the HFB Hamiltonian in a restricted space of canonical states orbitals³.

We have performed HFB+THO calculations for the Mg chain using our new HFB+THO prescription and with the same hamiltonian as used in Ref. ⁶). In Fig. 2, we compare our results with those of Ref. ³) in for nuclear deformations, quadrupole moments, rms radii and two-neutron separation energies. From the comparison, we see that our HFB+THO results are in perfect agreement with the coordinate results⁶ for the entire Mg chain.

4 Drip-line-to-drip-line calculations

Having tested the new HFB+THO procedure and shown that it very accurately reproduces all known results from the coordinate-space approach, we can now begin to use it as a tool for detailed investigations of nuclei across the periodic chart. Recently, we have performed systematic axially-deformed HFB+THO calculations for all even-even nuclei from the proton drip-line to the neutron drip-line with proton numbers $Z = 4, 6, 8, \dots, 104$. To clarify the role of the pairing force, we have performed the calculations with both volume and surface pairing. The analysis of the large array of data for these nuclei (more than 7500) is presently under way.

5 Acknowledgments

This work has been supported in part by the Bulgarian National Foundation for Scientific Research under project G-809, by the Polish Committee for Scientific Research (KBN), by the U.S. Department of Energy under Contract Nos. DE-FG02-96ER40963 (University of Tennessee), and DE-AC05-

OOOR22725 with. UT-Battelle, LLC (Oak Ridge National Laboratory), and by the US National Science Foundation under grant # PHY-99'70749.

References

1. E. Roeckl, Rep. Prog. Phys. **55**, 1661 (1992); A. Mueller and B. Sherrill, Annu. Rev. Nucl. Part. Sci. 43, 529 (1993); P.-G. Hansen, Nucl. Phys. A553, 89c (1993); J. Dobaczewski and W. Nazarewicz, Phil. Trans. R. Soc. Lond. A 356, 2007 (1998).
2. J. Dobaczewski, H. Flocard, and J. Treiner, Nucl. Phys. **A422**, 103 (1984); J. Dobaczewski, W. Nazarewicz, T.R. Werner, J.-F. Berger, C.R. Ghinn, and J. Dechargé, Phys. Rev. **C53**, 2809 (1996); A. Bulgac, Preprint FT-194-1980, Central Institute of Physics, Bucharest, 1980; nucl-th/9907088.
3. J. Terasaki, H. Flocard, P.-H. Heenen, and P. Bonche, Nucl. Phys. **A621**, 706 (1997); N. Tajima, XVII RCNP International Symposium on Innovative Computational Methods in Nuclear Many-Body Problems, eds. H. Horiuchi et al. (World Scientific, Singapore, 1998) p. 343; V.E. Oberacker and A.S. Umar, Proc. Int. Symp. on Perspectives in Nuclear Physics, (World Scientific, Singapore, 1999), Report nucl-th/9905010.
4. M.V. Stoitsov, W. Nazarewicz, and S. Pittel, Phys. Rev. **C58**, 2092 (1998); M.V. Stoitsov, P. Ring, D. Vretenar, and G.A. Lalazissis, Phys. Rev. **C58**, 2086 (1998); M.V. Stoitsov, J. Dobaczewski, P. Ring, and S. Pittel, Phys. Rev. C 61 (2000) 034311.
5. I.Zh. Petkov and M.V. Stoitsov, Compt. Rend. Bulg. Acad. Sci. 34, 1651 (1981); Theor. Math. Phys. 55, 584 (1983); Sov. J. Nucl. Phys. 37, 692 (1983); M.V. Stoitsov and I.Zh. Petkov, Ann. Phys. (NY) 184, 121 (1988); I.Zh. Petkov and M.V. Stoitsov, Nuclear *Density Functional Theory*, Oxford Studies in Physics, (Clarendon Press, Oxford, 1991).
6. J. Terasaki, P.-H. Heenen, H. Flocard, and P. Bonche, Nucl. Phys. A600, 371 (1996).